

18<sup>th</sup> ICCRTS

Agile Information Exchange in Autonomous Air Systems

Topics

Primary:

Topic 5: Experimentation, Metrics and Analysis;

Alternates:

Topic 8: Networks and Networking

Topic 11: Autonomy

David Scheidt

The Johns Hopkins University Applied Physics Lab, 11100 Johns Hopkins Rd, Laurel MD 20723

Kevin Schultz

The Johns Hopkins University Applied Physics Lab, 11100 Johns Hopkins Rd, Laurel MD 20723

Blair Chisholm

Atholton High School, 6520 Freetown Rd, Columbia, MD 21044

Point of Contact

David Scheidt

The Johns Hopkins University

Applied Physics Laboratory

11100 Johns Hopkins Rd

Laurel, MD 20724

David.Scheidt@jhuapl.edu

# Agile Information Exchange in Autonomous Air Systems

David Scheidt, Kevin Schultz, Blair Chisholm  
Johns Hopkins University Applied Physics Laboratory  
Laurel, MD  
{david.scheidt, kevin.schultz, blair.chisholm}@jhuapl.edu

**Abstract**— When the quality of service (QoS) of an unmanned air vehicle’s (UAV) communications link is poor, and the UAV is tracking a moving target, a trade-off exists between the fidelity and timeliness of information provided from the vehicle to an operator. The authors’ 2011 ICCRTS paper showed that an optimal representation scheme for transmitting information from UAV to operator can be found by using information theory. This paper extends that work by introducing an adaptive, autonomous unmanned air vehicle (UAV) command and control system that autonomously changes the fidelity of information communicated to an operator in response to variances in communications QoS. Results and analysis of hardware in-the-loop experiments using a UAV that is tracking a moving car are presented. This paper also examines the impact of information decay and network performance on both human tele-operation and on-board autonomous control, comparing the relative performance of tele-operation and autonomy as a function of *entropic drag*, which is a measurement, in information theory “bits”, of the rate at which information is lost due to unpredictable change in the environment. In the experiments described in this paper entropic drag is produced by the movement of the vehicle being tracked.

**Keywords**- *Networks and Networking; Agile Command and Control; Unmanned Vehicles; Autonomous Systems*

## I. INTRODUCTION

*“Imagine a world where sensors from seabed to space enable virtual operations from cyber-enabled warriors, and the speed of war is milliseconds.”* – CNO SSG XXVI [1]

The Command and Control Research Program (CCRP) has concluded that next generation war fighters will become increasingly “agile” [2], accelerating their observe, orient, decide and act (OODA) cycle by empowering “edge” units to make local decisions based upon “commanders intent”. Agile warriors are effective because, as CCRP correctly points out, the optimality of a decision or plan is frequently less important than the timeliness of the decision. Information timing *requirements* are dictated by operational tempo while information timing *capability* (derived from processing and

distribution latencies) is dictated by a combination of operational complexity and signal-to-noise ratio. Both operational tempo and operational complexity change constantly throughout an engagement, creating a dynamic interplay between information requirements and information capability. Agile war fighters will require supporting systems that use an understanding of this relationship to continuously adjust the flow of information in response to war fighter needs. The US military currently relies upon unmanned air systems to provide a large portion of tactical intelligence, surveillance and reconnaissance (ISR). The tactical information provided by UAVs is often dynamic, that is, the validity of the information changes due to unpredictable change in the environment being observed. The rate of change can vary from minutes, to milliseconds. The command and control systems currently used to control these platforms are not agile. A mismatch exists between our war fighters, who are capable of agile operations; and ISR systems that support them, which rely upon temporally insensitive *a priori* processes to control vehicle movement and information exchange vehicles.

This paper describes an agile information exchange mechanism between a single UAV and an operator. The goal UAV system is to retain track on a moving vehicle. The vehicle is prone to unanticipated course changes that introduce entropy into prior information provided by the UAV. As shown in Figure 1, for a fixed bandwidth, an optimal fidelity of information exists for exchanging information on a dynamic scenes that lose information due to a constant entropic drag. When the communications bandwidth between the UAV and user and/or the rate at which unpredictable acts cause prior knowledge to decay change, the optimal fidelity of information sent from the UAV to the operator (shown as the minima in Figure 1) changes. The current effective bandwidth and the entropic drag are measurable in real time. The information exchange mechanism uses real-time measurements of communications bandwidth and entropic drag to identify the optimal fidelity of ISR data. When the optimal fidelity is less than the maximum fidelity of the UAV’s on-board sensors, the information exchange system autonomously compresses sensor data, transmitting the compressed, lower fidelity data to the user. Because the lower-fidelity data requires fewer bits to transmit the data is received by the user sooner, the information loss due to entropic drag is

less and, importantly, the combined information loss due to compression and entropic drag is minimized.

The next section of this paper describes theoretical basis for autonomous data compression as a function of communications bandwidth and entropic drag. That section is followed by a section describing a practical experiment in which a real UAV used on-board bandwidth measurements to vary the fidelity of track imagery communicated to the user.

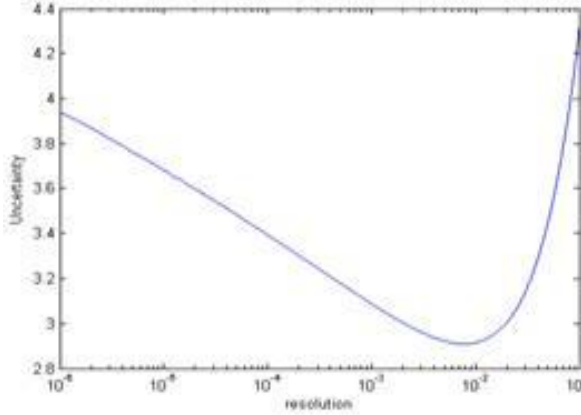


Figure 1: Uncertainty of a sample two-dimensional world showing effects of entropic drag as unit resolution is increased. Increasing resolution increases complexity, which increases communication time, resulting in more entropic drag [3].

## II. THEORY

This section reviews the authors' previous work on the application of information theoretic concepts to command and control and applies them to the overhead-tracking scenario with limited communications bandwidth.

### A. Definitions

Suppose that the C2 process  $x(t)$  operates in a discrete state space  $X = \{x_i\}$  with finite cardinality  $|X|$ . The discreteness of the state space is not absolutely required, as long as the sensor discretizes the output in an appropriate fashion. The number of bits required to describe the state is the *descriptive* complexity and it is equal to  $\log_2|X|$ . This quantity can be thought of as the fidelity to which the C2 process is described, e.g., to the nearest meter as compared to kilometer.

To ascribe a notion of uncertainty and information to the C2 process, Shannon information entropy is used. The information entropy  $H$  of the process  $x$  at time  $t$  is

$$H(x(t)) = -\sum P(x_i, t) \log_2(P(x_i, t)),$$

Where  $P(x_i, t)$  is the probability that the process  $x$  is in state  $x_i$  at time  $t$ . Given a specific observation of the process  $x(t) = x_i$ , the information  $I$  is

$$I(x_i, t) = -\log_2 P(x_i, t).$$

Thus, one interpretation of entropy is the expected information gain of an observation. It is also known that entropy is maximized when all states of the system are equally probable,

and so the descriptive complexity is also the maximum possible entropy of the system, given a fixed discretization.

Suppose we have an observation  $S = (x_i, t)$ , meaning through an observation we have  $x(t) = x_i$ . Using the definition above (as well as an abuse of notation) yields

$$I(S, t) = -\log_2 P(x_i, t).$$

Note that the second argument above is a time index as well. As time elapses the relevance of the observation  $S$  should decrease, and it is natural to ask what information the observation  $S$  has about  $x(t')$  for some  $t' > t$ . If the system is not uniquely determined by a single observation, then the conditional expected information content of a second observation  $S' = (x_j, t')$  of the same sensor at a later time  $t'$  is  $H(x(t')|S) = H(x(t')|x(t) = x_i)$ , and this is defined similarly to  $H(x(t))$  but using the conditional probability distribution  $P(x_j, t'|x(t) = x_i)$ . The very fact that repeating the same observation results in the gain of new information beyond the original observation indicates that the prior observation's information content has in some sense decayed.

For a sequence of  $k$  observations  $S_{1:k} = \{(x_j, t_j)\}$  of the process  $x$  with the final observation at  $t_k = t$ , the *entropic drag*  $\Gamma$  of the system on the observations  $S_{1:k}$  at time  $t' > t$  is

$$\Gamma(S_{1:k}, t, t') = \frac{H(x(t')|S_{1:k})}{t' - t}.$$

Conceptually, entropic drag can be thought of as the time derivative of conditional entropy, but in a strict mathematical sense the assumed discrete space will not admit a derivative. For observations that occur with fixed sampling time  $\Delta t$  the quantity  $\Gamma(S_{1:k}, t, t + \Delta t)$  is effectively the expected rate of information generation of the system at time  $t$ . This notion can be generalized to multiple sensors [4]. However, entropic drag should not be interpreted solely as the change of state of the underlying system as predictable change should have significantly lower entropic drag (if any at all) as compared to systems whose change is less predictable.

### B. Analysis

In [5], the notion of entropic drag was defined for a simple tracking problem on a grid with noiseless sensors that can measure the entire grid at once. In this framework,  $x(k)$  is the location of the a single target in the state space  $X$ . Given a purely Markovian motion model and an initial probability distribution  $P(x_j, k)$ , one can compute the probability distribution on state using the relationship

$$P(x_i, k + 1) = \sum_{x_j \in X} P(x_j, k) P_{x_j}(x_i), \quad (1)$$

where  $P_{x_j}(x_i)$  is the probability that the target moves to  $x_i$  given it is currently in  $x_j$ . Using this equation, it was demonstrated that the effects of entropic drag varied with the specifics of the motion model  $P_{x_j}(x_i)$ . Here, we consider a different analysis of entropic drag. Instead of varying the motion model, the sensor granularity will be varied. By reducing the granularity of the sensor, the initial observation is less informative, but the number of bits required to describe an

observation will be fewer. If these observations are transmitted over a noiseless communications channel with bitrate  $r$ , then an observation that requires fewer bits to encode will require less time to transmit, and thus will be subject to entropic drag for a shorter amount of time. This could potentially result in a more informative observation *after* transmission.

Suppose we setup the state  $X$  for the tracking of an object on an  $N \times N$  grid, with circular boundary conditions for simplicity. Clearly, the descriptive complexity in this scenario is  $2 \log_2 N$ . Furthermore, suppose that the object being tracked can make a move to any of eight adjacent grid squares (including diagonals), or stay put, every  $T_s$  seconds. We have at our disposal a finite number of sensing options  $i$  that can quantize the underlying  $N \times N$  grid by a factor of  $q_i$ . For purposes of simplicity, we will assume that  $N$  is a power of 2, and that  $q_i = 2^i$ . So, the number of bits required to encode an observation using quantization factor  $q_i$  is

$$\log_2 \left( \frac{N \times N}{q_i \times q_i} \right) = 2 (\log_2 N - 2 \log_2 q_i). \quad (2)$$

From the above expression it is clear that reducing the resolution of the sensor by a linear factor reduces the number of possible values of the sensor by a quadratic factor, but only reduces the communications time by a linear factor. We will revisit the implications of this observation later, but for now we continue with the calculation of the entropic drag based on the bitrate  $r$  and the quantization factor  $q_i$ .

What then is the information theoretic impact of using sensing option  $i$ ? Well, just because we have coarsened the observations taken does not mean that the underlying motion or state model of the target should change. The target should still move on the  $N \times N$  grid every  $T_s$  seconds. When an observation is taken, it encodes this observation into the coarser  $\frac{N}{q_i} \times \frac{N}{q_i}$  grid. The approach considered here to incorporate this coarser measurement with the finer grid where the motion model (and thus entropic drag) is defined, is to refine the observation to the finer grid using a maximum entropy approach. Put simply, given a coarse observation we know this means that the target was detected in a unique  $q_i \times q_i$  square in  $X$ . Using a maximum entropy approach, we assign the probability of target presence in each of those  $q_i^2$  locations to be  $1/q_i^2$ . Once an observation has been converted to a probabilistic state on  $X$ , calculating the entropic drag on an observation amounts to applying the motion model (1) for the number of target moves  $M$  that can occur in the time it takes to transmit the observation, as determined by the communications bitrate  $r$  and the descriptive complexity induced by sensor mode  $i$ , as determined by (2), that is

$$M = \left\lfloor \frac{2(\log_2 N - 2 \log_2 q_i)/r}{T_s} \right\rfloor.$$

As an example, Figure shows the information content of an observation for a tracking problem where  $N = 1024$  and  $q_i \in \{1, 2, 4, 8, 16, 32\}$ , as a function of the communications

bitrate  $r$ . Note that aside from some quantization issues, there are clear ranges of  $r$  where each of the quantization levels results in the maximum information content of the observation after transmission, i.e., minimum uncertainty. This example, while notional, clearly illustrates the tradeoffs between sensor resolution and uncertainty.

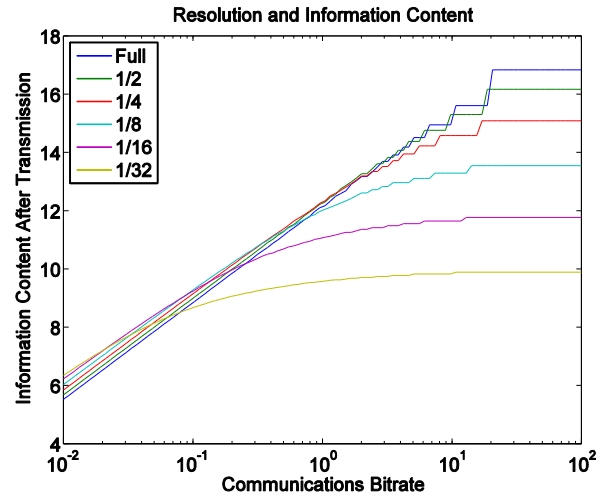


Figure 2: Information content after transmission as a function of quantization and communications bitrate.

As alluded to above, when the sensor quantization increases by a linear factor, the resolution of the sensor, say as an image, reduces by a quadratic factor. This decrease in resolution should eventually result in a decrease in detection probability,  $p_d$ , of the target, with continued quantization eventually resulting in a  $p_d$  of 0. Previously, the target detection probability was assumed to be 1, regardless of sensor modality. Clearly, if the probability of detection decreases, then the initial information content of the sensor observation (that is, prior to transmission and the effects of entropic drag) should alternate between 0 and the value in (2), depending on whether or not that observation resulted in a detection or not. To calculate the entropic drag in such a scenario is essentially equivalent to ignoring the sensor observations that did not result in detection and continuing to apply the motion model (1) until a new detection is received. Additionally, an  $N \times N$  image that uses  $B$  bits of color/intensity information per pixel requires  $2B \log_2 N$  bits to encode an observation from which a maximum  $2 \log_2 N$  bits of information about the target's location can be derived. This begins to illustrate the subtle point that maximizing raw information may not be the ideal objective function to consider when applying information theoretic concepts to C2 problems, and instead one should consider other notions of utility as mentioned in [6]. For a tracking problem, a reasonable metric to consider should be one that attempts to characterize the notion of maintaining a persistent track, perhaps by not allowing a lapse in detection of length greater than  $L$  seconds.

The metric we will use in this slightly more realistic tracking scenario (that is, the scenario with  $p_d < 1$ ) is the probability that the track will be continued given an initial detection, i.e., given a successful detection, another successful detection will occur with  $L$  seconds. Given the probability of detection  $p_d$ , which here will be a function of image resolution only. This metric can be defined using the cumulative distribution function of a geometric distribution with parameter

$$p_c = 1 - (1 - p_d)^{\lfloor L/T \rfloor},$$

where  $T = B \left( \frac{N^2}{q_i^2} \right) / r$ , the amount of time that it takes to transmit an  $N \times N$  image with pixel depth  $B$  using quantization factor  $q_i$ . For typical cameras,  $B = 8$  for grayscale images and 24 or 32 for color. This assumes, however, that the image is not compressible. In practice, the images captured by such a device are highly compressible (that is, they contain much less information than the number of pixels and bit-depth would indicate) as indicated by the file sizes of the experimental setup below. Furthermore, this compression level could also be a parameter to select from, in much the same way as image resolution. So, for the purposes of analysis and algorithm development, we will use the empirical file sizes generated by the experimental setup, which ranged between 128 to 239 kb over four levels of resolution, which is far less than the 192 Mb one would expect naively from the 8 megapixel images considered.

Figure shows how the probability of track continuation varies as the time delay between observations (which may include missed detections) for various  $p_d$ . This plot is not particularly interesting since it does not tie the notion of detection probability with the delay in observation time. Put simply, if the time delay between observations is fixed and independent of  $p_d$ , one would naturally select the sensor modality that maximized  $p_d$ . Figure 4 shows the far more interesting case, when observation time delay and  $p_d$  are both functions of the image quantization factor  $q_i$ . For these plots, the  $p_d$  values correspond by color to the values used in Figure 3. It is clear from Figure 4 that for each communication's bitrate, there is an optimum quantization factor, in terms of track continuation, and the optimum  $q_i$  varies with  $r$ . Thus, if one were able to reliably estimate  $r$ , one could use determine the optimal quantization factor  $q_i$  to maximize  $p_c$ .

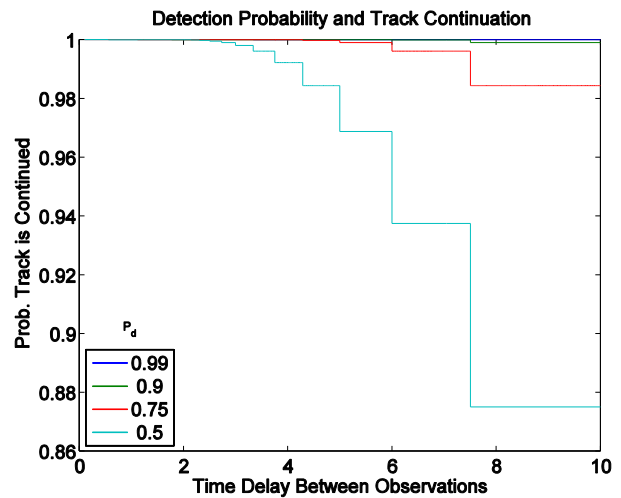


Figure 3: Track continuation as a function of detection probability and observation frequency.

Of course, there are some disclaimers in this analysis that need to be considered, but the general principles should remain valid, but may require simulation and experimentation (instead of closed-form calculation) to derive. First, the specific values of  $p_d$  used here are notional as are the bitrates and descriptive complexities. To actually compute the probability of detection given a set of image factors requires substantial testing and is likely application specific. Furthermore, since modern image formats use compression to reduce file size, potentially complicating the calculation of transmission time. This is somewhat mitigated, however, by the expectation that since the background image should remain relatively constant, the compression level should remain relatively fixed. This notion could be exploited (as it often is in movie compression) to only encode the “changes” between images to reduce the amount of information transmission required. Additionally, the true transmission time should include both latency (from the sensor and the communications channel), although incorporating these (at least in the deterministic, expected, or worst case) should be straightforward and depend on whether the observations are pipelined (in which case the latency is irrelevant) or if the observations are on demand (in which case they should add in to the total transmission time).



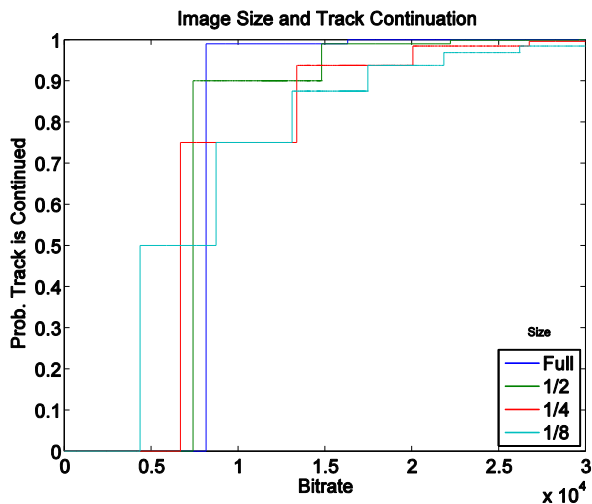


Figure 4: Track continuation as the image resolution and communication's bitrate varies.

### III. EXPERIMENTATION

#### A. Use Case

Our experimental concept of operations (CONOPS) is a simple target tracking problem in which a single UAV provides target imagery to a single user. UAVs collect more data than can be transmitted in time to be useful. This is especially true in communications challenged environments including: intentional interference (e.g., jamming), changing environmental conditions, changing network usage or crosstalk with other electromagnetic systems.

The adaptive system presented would keep fidelity as high as possible while sending images at a rate that would keep the target in the field of view. In this problem the speed of the target and the bandwidth available for communication between the UAV and the operator can be determined. Fidelity of the images sent to the operator can be varied to increase the probability of maintaining track. An Android app was developed to test the change in bandwidth over time and in response to file size and signal strength. It sent images with file sizes between 128 and 239 kb. The time that the message was sent and received and the signal strength at the time it was sent were recorded. As would be expected, bandwidth decreases quickly with worsening signal strength.

#### B. Metrics

As described in the previous section, the goal of the target tracking UAV is to maximize the probability of detection,  $p_d$ , and, once the target has been detected, maximize the probability of track continuation,  $p_c$ , which we assume is a function of image resolution only.

#### C. Assumptions

Our experiment makes several simplifying assumptions, which are:

- Target vehicle behavior is completely unpredictable, this allows us to conveniently, yet unrealistically, assume that all feasible trajectories are equally probable. For a more

nuanced dissertation on post observation target trajectory probability distribution see [7].

- The information provided by imagery decays in proportion to the localization accuracy. While this is true for track continuation, this is not true for target detection and target classification.
- The decision-making process of the pilot was not modeled, rather, we assume that the ability of the pilot to track the target is proportional to the information the pilot has on the target.

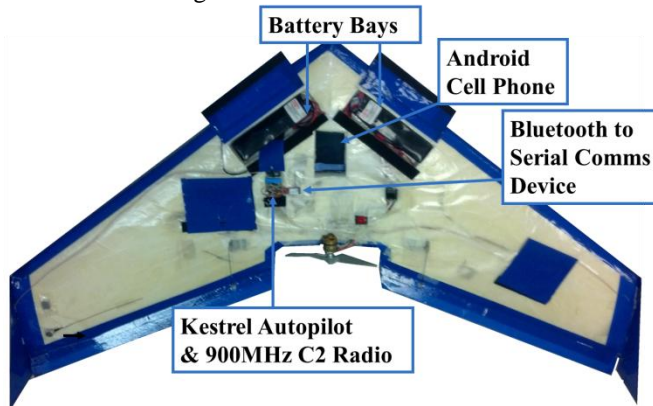


Figure 5: Modified Procerus Unicorn UAV

#### D. Equipment

The UAV used in this experiment is a modified Procerus Unicorn (Figure 5). Unicorns are electrically powered, Styrofoam flying wings with a 72" wingspan. Stock Unicorns are controlled by a Kestrel autopilot, which communicates to a ground-station over a 900MHz radio link. Through the ground-station, the Unicorn operator can control the Unicorn with simple commands, such as loiter at this waypoint, land at this location, or fly this path. The Unicorn was modified to include a Samsung Galaxy S II cell phone running the Android 4.1.2 Jelly Bean operating system. The phone's reverse-face camera was used as a payload to provide target imagery. The phone was mounted with the camera unobscured and pointed down. Image metadata that described the time and location of the image was provided by the GPS receiver integrated into the phone.

The UAV was configured for tele-operated control, following waypoints provided by the stock Unicorn ground-station, and as an autonomous unmanned vehicle. When operating autonomously waypoint commands were sent from the autonomy toolkit (ATK) software running on the Android cell-phone over a Bluetooth wireless connection to the Kestrel autopilot. When operating autonomously ATK interprets position data from the phone's GPS data and payload sensors and devises a course that satisfies user-defined mission-level goals. A detailed description of ATK can be found in [8].

The communications network used in our experiments was the public AT&T public cell-phone network. The cell phone network provides a variable quality of service (QoS) mobile ad hoc network (MANET) whose available bandwidth varies

in response to overall network usage and signal strength. From the point of view of a single phone-to-phone data link the cell QoS variations are unpredictable, which allows us to use the cell network as a proxy for military wireless communications in contested areas. Using the AT&T network, target images are sent from the on-board cell phone to the operator’s Galaxy S II as attachments using email.

Test flights were conducted at an altitude of 300-400ft. This altitude was selected to comply with flight safety regulations and also to provide target imagery of a size that is amenable to both manual and automated target detection. A sample image is shown in Figure 6.



Figure 6: Imagery from the cell phone camera tracking a white van down a country road.

### E. The Agile Information Exchange Algorithm

A simple information exchange protocol was used to adjust the rate and quality of images sent from the UAV phone to the operator phone. The algorithm sends messages continuously, one after another without delay, as soon as the previous message has been received. The frame rate at which the phone can capture images far exceeds the rate at which they can be transmitted across the cell network. To prevent multiple images from queuing up inside the network, which produces latency-induced entropy, images are taken and sent only when the prior image has been sent to the email server. This strategy produces a frame rate of the image file size divided by the bit rate.

The algorithm varies the image quality in order to maintain a delay between images that is smaller than a specified time,  $T_{max}$ , while sending the highest quality images possible. For experiments here,  $T_{max}$  was set to 9.09 seconds, which was computed to be an upper bound on the time required to keep a slow moving vehicle in scene. By measuring the send-receive time for a message of known size, the algorithm is able to estimate the current it rate provided by the network. This time is averaged over a small number of consecutive messages (here, a value of five is used) to produce a smoother estimate of the bandwidth. The algorithm then uses a look-up table derived from previous experiments to estimate the typical file sizes for a given resolution and compression factor, and then

looks for the highest quality settings such that the average file size divided by the current bandwidth estimate is less than  $T_{max}$ . The average file size could be replaced by a larger quantity in order to hedge against randomness in file sizes if necessary. Alternatively, using a smaller  $T_{max}$  would result in similar a similar effect.

Originally, it was envisioned that the phone’s signal strength sensor would be used to determine the image quality settings in the agile exchange algorithm, however, baseline experimentation indicated that the signal strength was not strongly correlated with the computed bandwidth during message transmission (see Figure 7), making it an unreliable estimator. Thus, using the recent history of bandwidth was the only available data. Even this was quite noisy, so the average over several messages is used in order to low-pass filter the bandwidths,

### F. Results

#### 1) Communications baseline

For the agile information control algorithm to be of value two assertions on network characteristics must hold. These assertions are:

1. Network QoS must vary over the course of an engagement.
2. The rate at which network QoS varies must be significantly less than the time required to send an image.

Prior to flight testing, experiments were conducted to characterize the cell phone network. As indicated in the scatter plot shown in Figure 7, the time required to send images of varying size varied considerably, indicating that assertion #1 is valid. As indicated by the time-series plot in Figure 8, the rate at which network QoS varies is slower than the time required to end a single image.

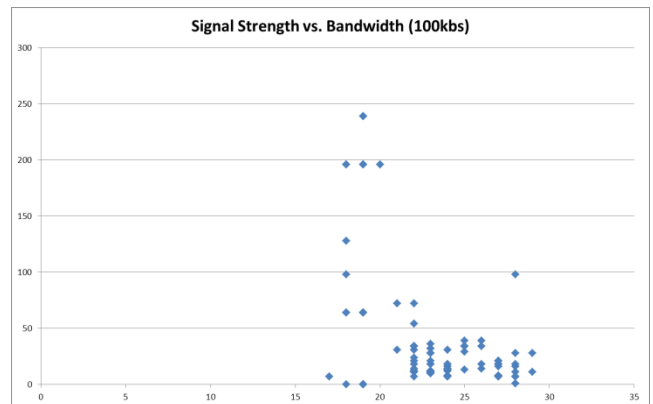


Figure 7: Signal strength vs. bandwidth

#### 2) Flight test results

Unfortunately, actual flight tests using the information exchange algorithm resulted in some unexpected phenomenon that render the algorithm ineffective, at least using the

hardware and imaging used here. Figure 9 shows a plot of the bandwidth (i.e., the ratio of image size to image sending time) over time. The 'x' marks indicate the time that the actual message was sent, with the lines present simply to illustrate the shape of the curve. Clearly, there is a strong periodic component present in the bandwidth that was not present for measurements taken on the ground. Since the UAV was fixed wing and it cannot hover over a target, it must loiter in a circular pattern, and we conclude that it is this periodic motion is inducing the periodic behavior in the bandwidth. We further conjecture that this is not a function of a change in distance between the UAV and the nearest cell tower that is causing this change in bandwidth, but rather a change in orientation of the cell phone with regards to the cell tower, resulting in changes in performance due to directionality in the antenna, or through asymmetries in the airframe affecting electromagnetic propagation.

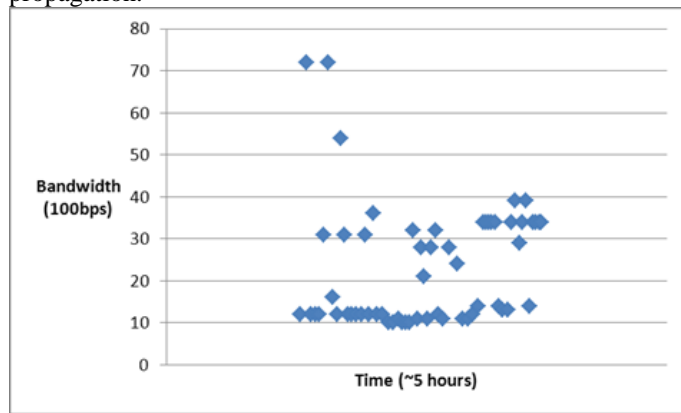


Figure 8: Time series plot of bandwidth

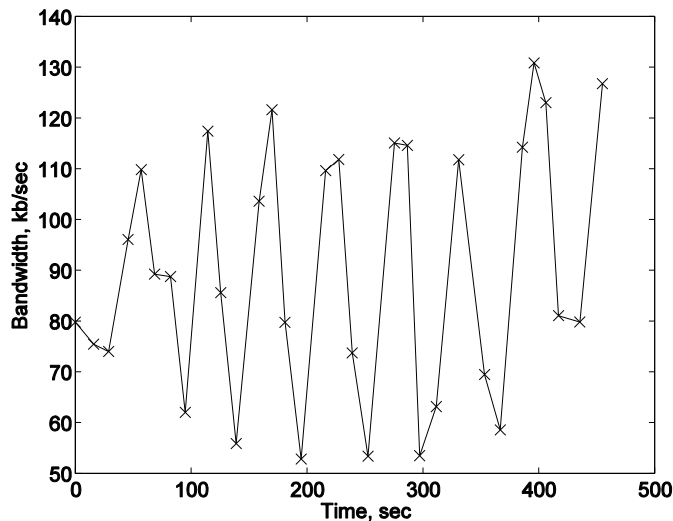


Figure 9: Bandwidth over time during a single flight experiment.

If the observed periodicity were much slower than the rate at which the information exchange algorithm was able to transmit imagery, these smooth changes in bandwidth would have been handled by the algorithm. However, as noted before, the information exchange algorithm updated its

estimate of the bandwidth every three images, which appears to be around the period of the bandwidth change. This is reflected in Figure 10, where the time between messages varies considerably and is often over the desired rate of one image per 9.09 seconds. This is due to the image compression settings not being compatible with the actual bandwidths.

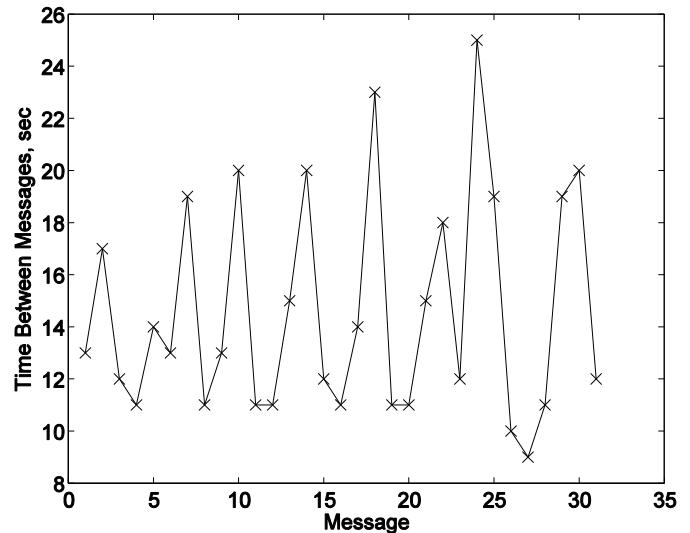


Figure 10: Delay between consecutive messages in a single flight experiment.

Alternatively, it may be possible to improve performance in the algorithm if position and trajectory information were included in the predictions of bandwidth. Unfortunately, the aircraft heading and waypoint information is inaccessible to the cell phone, but the cell phone's GPS may have some useful information that could be incorporated. One could envision an algorithm that builds up correlations between position and bandwidth that could prove useful in an urban environment, for example.

#### IV. CONCLUSION

This paper describes a prototype agile information exchange system for exchanging information between a UAV and a UAV operator. The information exchange system uses real-time information-theoretic measurements of the operating environment and the communications infrastructure to adjust the fidelity of data being communicated from the UAV to the operator. The theoretical basis that is used by system to adjust data fidelity is explained and an analysis of the potential benefits is provided.

A prototype information exchange system that includes a single, research-grade UAV communicating to an operator over the public cell-phone network is described. Laboratory-based characterizations of the cell phone network and flight test results of the modified UAV using the agile information exchanging system to provide imagery of a moving target are provided. However, the immediate utility of such a system is significantly decreased due to an unexpected interaction between the motion of the UAV and the bandwidth.



#### ACKNOWLEDGMENT

This research was performed APL Student Program to Inspire, Relate and Enrich (ASPIRE) program that places gifted and talented high school students into mentoring relationships with APL staff members to complete research projects. The authors would like to thank Jon Castelli, of JHU/APL and Ryan Freeburger, an ASPIRE student from Century High School, for UAV preparation and flight operations.

#### REFERENCES

- [1] J. R. Hogg, The Convergences of Sea Power and Cyber Power (video), Chief of Naval Operations Strategic Studies Group XXVI, March 2008.
- [2] D. Alberts, R. Hayes, Power to the Edge, CCRP Press, 2003.
- [3] D. Scheidt & M. Pekala, "The Impact of Entropic Drag on Command and Control," *12th ICCRTS : Adapting C2 to the 21st Century*. Newport, RI: DoD Command and Control Research Program, 2007.
- [4] K. Schultz, "Towards Agile Control of Ship Auxiliary Systems," *4<sup>th</sup> International Symposium on Resilient Control Systems*, 2011
- [5] K. Schultz and D. Scheidt, "An Application of Information Theory to Command and Control," *17<sup>th</sup> ICCRTS*, 2012
- [6] D. Scheidt and K. Schultz, "On Optimizing Command and Control Structures," *16<sup>th</sup> ICCRTS*, 2011.
- [7] A. Shem, "An Analytic Model to Evaluate the Influence of Uncertainty on the Cooperative Search Behaviors of Autonomous UAVs," PhD dissertation, School of Engineering and Applied Science, George Washington University, March 6, 2006.
- [8] D. Scheidt, "Organic Persistent Intelligence Surveillance and Reconnaissance," *JHU/APL Technical Digest*, Volume 34, Number 1, Jan 2013.